Loss of PWT7, Located on a Supernumerary Chromosome, Is Associated with Parasitic Specialization of Pyricularia oryzae on Wheat

Asuke, Soichiro ; Horie, Akiko ; Komatsu, Kaori ; Mori, Ryota ; Vy, Trinh Thi Phuong ; Inoue, Yoshihiro ; Jiang, Yushan ; Tatematsu, Yuna ⋯

(Citation)
Molecular Plant-Microbe Interactions,36(11):716-725

(Issue Date)
2023-11

(Resource Type)
journal article

(Version)
Version of Record

(URL)
https://hdl.handle.net/20.500.14094/0100485940

MPMI Vol. 36, No. 11, 2023, pp. 716–725, https://doi.org/10.1094/MPMI-06-23-0078-R

Loss of *PWT7*, Located on a Supernumerary Chromosome, Is Associated with Parasitic Specialization of *Pyricularia oryzae* on Wheat

Soichiro Asuke,[1] Akiko Horie,[1] Kaori Komatsu,[1] Ryota Mori,[1] Trinh Thi Phuong Vy,[1] Yoshihiro Inoue,[2] Yushan Jiang,[1] Yuna Tatematsu,[1] Motoki Shimizu,[3] and Yukio Tosa[1,†]

[1] Graduate School of Agricultural Science, Kobe University, Kobe 657-8501, Japan
[2] Graduate School of Agriculture, Kyoto University, Kyoto 606-8502, Japan
[3] Iwate Biotechnology Research Center, Kitakami, Iwate 024-0003, Japan

Accepted for publication 8 July 2023.

Pyricularia oryzae*, a blast fungus of gramineous plants, is composed of various host genus–specific pathotypes. The avirulence of an *Avena* isolate on wheat is conditioned by *PWT3* and *PWT4*. We isolated the third avirulence gene from the *Avena* isolate and designated it as *PWT7*. *PWT7* was effective as an avirulence gene only at the seedling stage or on leaves. *PWT7* homologs were widely distributed in a subpopulation of the *Eleusine* pathotype and the *Lolium* pathotype but completely absent in the *Triticum* pathotype (the wheat blast fungus). The *PWT7* homolog found in the *Eleusine* pathotype was one of the five genes involved in its avirulence on wheat. A comparative analysis of distribution of *PWT7* and the other two genes previously identified in the *Eleusine* pathotype suggested that, in the course of parasitic specialization toward the wheat blast fungus, a common ancestor of the *Eleusine*, *Lolium*, *Avena*, and *Triticum* pathotypes first lost *PWT6*, secondly *PWT7*, and, finally, the function of *PWT3*. *PWT7* or its homologs were located on core chromosomes in *Setaria* and *Eleusine* isolates but on supernumerary chromosomes in *Lolium* and *Avena* isolates. This is an example of interchromosomal translocations of effector genes between core and supernumerary chromosomes.

Keywords: avirulence gene, *Magnaporthe oryzae*, minichromosome, *Pyricularia oryzae*, supernumerary chromosome, wheat blast

Pyricularia oryzae (syn. *Magnaporthe oryzae*), a blast fungus of gramineous plants, is composed of host genus–specific subgroups such as the *Oryza* pathotype (MoO), *Setaria* pathotype (MoS), *Eleusine* pathotype (MoE), *Lolium* pathotype (MoL), and *Triticum* pathotype (MoT), which are pathogenic to rice, foxtail millet, finger millet, perennial ryegrass, and wheat, respectively (Cruz and Valent 2017; Kato et al. 2000; Tosa et al. 2004). Each pathotype forms a distinct lineage in a phylogenetic tree of *P. oryzae* isolates, except that the MoE is divided into two sublineages, *Eleusine* 1 and *Eleusine* 2 (Gladieux et al. 2018) or EC-I and EC-II (Asuke et al. 2020a). The *Lolium* lineage includes a unique isolate, Br58, which is pathogenic on oats but nonpathogenic on hosts of the pathotypes mentioned above (Gladieux et al. 2018; Oh et al. 2002). This isolate is considered to be on evolutionary processes toward an *Avena* pathotype (MoA). In this article, we will regard Br58 as MoA. To elucidate genetic mechanisms of the pathotype-genus specificity, Takabayashi et al. (2002) crossed Br58 with MoT isolate Br48 and identified two genes, *PWT3* and *PWT4*, conditioning avirulence of Br58 on wheat. They also identified a resistance gene corresponding to *PWT4* and designated it as *Rmg1* (*Rwt4* listed as a synonym). A subsequent cross of MoL isolate TP2 with Br48 revealed that the avirulence of TP2 on wheat is mainly conditioned by *PWT3* (Inoue et al. 2017; Vy et al. 2014). A resistance gene corresponding to *PWT3* was identified and designated as *Rmg6* (*Rwt3* listed as a synonym) (Inoue et al. 2017; Vy et al. 2014). These results suggested that the pathotype-genus specificity is under the control of gene-for-gene interactions.

MoT, the causal agent of wheat blast, first emerged in Brazil in 1985 and then spread to neighboring countries in South America (Singh et al. 2021; Urashima et al. 1993). In the 2010s, it was transmitted to Asia and Africa independently (Latorre et al. 2023; Singh et al. 2021) and caused severe outbreaks of wheat blast in Bangladesh (in 2016) and Zambia (in 2018), respectively (Islam et al. 2016; Tembo et al. 2020). Currently, wheat blast is about to become a pandemic disease that threatens world wheat production. To elucidate molecular mechanisms of the evolution of MoT, Inoue et al. (2017) cloned *PWT3*, which is ubiquitous in MoL, and showed that the disruption of *PWT3* in TP2 (MoL) resulted in the gain of virulence on wheat. Based on this result and a historical record of wheat cultivation in Brazil, they suggested that the host jump of *P. oryzae* to wheat occurred through two steps: (i) wide cultivation of a *pwt3* cultivar or cultivars enabled MoL or its close relatives carrying *PWT3* to colonize and adapt to common wheat; (ii) subsequent functional losses of *PWT3* resulted in the emergence of MoT pathogenic on the entire common wheat population.

In these analyses, we have used cultivar Hope as a control, i.e., as an exceptional common wheat cultivar lacking both *Rwt3* and *Rwt4*. Hope was susceptible to MoL isolate TP2 (*PWT3*; *pwt4*)

[†]Corresponding author: Y. Tosa; tosayuki@kobe-u.ac.jp

S. Asuke, A. Horie, and K. Komatsu contributed equally to this work.

Nucleotide sequence data reported here are available in the DDBJ, EMBL, and GenBank databases under accession numbers PRJDB14584 and PRJDB14749.

Funding: This research was supported by a grant-in-aid for scientific research from the Japan Society for the Promotion of Science 21H04726.

e-Xtra: Supplementary material is available online.

The author(s) declare no conflict of interest.

at the seedling and heading stages, as expected. Against Br58 (*PWT3*; *PWT4*), however, Hope was susceptible at the heading stage but resistant at the seedling stage. These results suggested that the Br58-Hope interaction involved an additional avirulence gene–resistance gene pair effective at the seedling stage alone. In this article, we report cloning of this new avirulence gene. Interestingly, this gene was located on supernumerary chromosomes in MoL and MoA isolates but on core chromosomes in MoE and MoS isolates. This result suggests that some avirulence genes involved in the pathotype-genus specificity underwent interchromosomal translocations between core and supernumerary chromosomes during the course of pathotype differentiation.

Results

Isolation of *PWT7*

To check whether the additional avirulence gene is involved in interactions with wheat cultivars other than Hope at the seedling stage, Br58Δ3Δ4 produced by Inoue et al. (2017) was sprayed onto primary leaves of common wheat cultivars, Norin 4 (N4) (carrying both *Rwt3* and *Rwt4*) and Chinese Spring (CS) (carrying *Rwt3* alone). In these interactions there should be no known matching gene pairs because Br58Δ3Δ4 is a disruptant of *PWT3* and *PWT4* derived from Br58. Although Br58Δ3Δ4 was virulent on spikes of N4 and CS (Inoue et al. 2017), it showed avirulence on their primary leaves (Table 1), suggesting that an additional gene pair other than *PWT3-Rwt3* and *PWT4-Rwt4* is involved in the incompatibility of Br58 with N4 and CS at the seedling stage. As a representative MoL isolate, we have used TP2 (*PWT3*; *pwt4*) (Inoue et al. 2017; Vy et al. 2014), which was virulent on Hope at the seedling and heading stages as mentioned above. N4 and CS were resistant to TP2 and susceptible to its *PWT3* disruptant (TP2Δ3) produced by Inoue et al. (2017) not only at the heading stage (Inoue et al. 2017) but also at the seedling stage (Table 1), suggesting that the reactions of TP2 with Hope, N4, and CS are explained by the *PWT3-Rwt3* interaction alone, irrespective of the growth stages. To check whether this is a general feature of MoL isolates or an exception, we employed four additional MoL isolates (TP1, AK1, LW3, and FI5). They had the same genotypes as TP2 at the *Pwt3* and *Pwt4* loci, i.e., *PWT3*; *pwt4*, but showed phenotypes different from TP2. They were avirulent on primary leaves of Hope (Table 1). Furthermore, their *PWT3*-disruptants (TP1Δ3, AK1Δ3, LW3Δ3, FI5Δ3) were all avirulent on N4 and CS (Table 1). Based on these results, we assumed that the avirulence gene effective at the seedling stage alone was widely distributed in isolates in the *Lolium* lineage, including the MoA isolate, and was effective on a wide range of common wheat cultivars, including Hope, CS, and N4.

To clone the gene (tentatively designated as *PWTX*) conditioning the avirulence of Br58 on Hope at the seedling stage, we produced a mapping population through backcrossing. Of the F_1 cultures derived from the cross between Br58 and Br48, we chose 76Q1 virulent on Hope (Table 1), crossed it with Br58, and obtained 167 BC_1F_1 cultures (Fig. 1). For rough mapping, 79 cultures were arbitrarily chosen and were sprayed onto primary leaves of Hope. Avirulent and virulent cultures segregated 21:58, although the ratio was deviated from an expected monofactorial segregation. Of the 21 avirulent cultures, we chose 18 showing stable phenotypes, extracted their genomic DNA, bulked them, sequenced, and aligned the sequence reads to the whole-genome sequence of Br58. Analyses with the single nucleotide polymorphism (SNP) index (Abe et al. 2012) and presence or absence polymorphisms led us to identify a candidate region (approximately 730 kb) harboring *PWTX*. Genes encoding proteins with secretion signals in this region were predicted, roughly picked up with intervals, and converted to PCR-based molecular markers. As a result of molecular mapping with the 79 BC_1F_1 cultures, we found that segregation of molecular markers was also distorted in this region. Furthermore, we found two markers with 100% linkage to *PWTX* (MOAC3166 and MOAC3013) and three flanking markers with 1 recombinant (MOAC3719, MOAS258, MOAS347) (Fig. 2A). These results indicate that the distortion of the segregation in phenotypes mentioned above is not due to involvement of more than one gene but should be attributed to some abnormal behaviors of chromosomes in meiosis. Since the

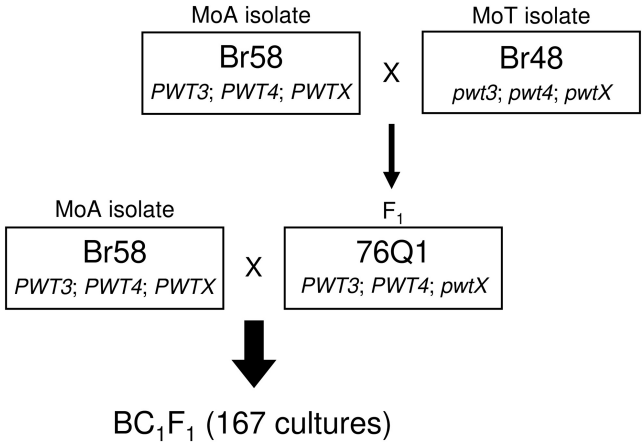

Fig. 1. Pedigree of *Pyricularia oryzae* strains used in this study.

Table 1. Wheat and barley cultivars used and their infection types with various isolates and strains of *Pyricularia oryzae* at the seedling stage

	Infection types[a] with *P. oryzae* isolates/strains[b]															
	Genotype		Br48	76Q1	Br58		TP2		TP1		AK1		LW3		FI5	
Species/cultivar	*Rwt3*	*Rwt4*	WT	F_1	WT	Δ3Δ4	WT	Δ3	WT	Δ3	WT	Δ3	WT	Δ3	WT	Δ3
Hordeum vulgare																
Nigrate (Ngt)	−	−	5G	5G	5G	5G	5G	5G	5G	5G	4-5G	4-5G	5G	5G	5G	5G
Triticum aestivum																
Hope	−	−	5G	5G	1B	1B	5G	5G	0	0	0	0	0	0	0	0
Norin 4 (N4)	+	+	5G	0	0	0	1B	5G	0	0-1B	0	0	0	0	0	0
Chinese Spring (CS)	+	−	5G	0	0	0	1B	5G	0	0	0	0	0	0	0	0

[a] 0 = no visible infection; 1 = pinhead spots, 2 = small lesions, 3 = scatterd lesions of intermediate size, 4 = large typical lesions, 5 = complete blighting of leaf blades. B and G represent brown and green lesions, respectively.

[b] Br48 = MoT isolate, Br58 = MoA isolate, 76Q1 = F_1 hybrid derived from Br58 × Br48, TP1, TP2, AK1, LW3, FI5 = MoL isolates. WT = wild type, Δ3 are disruptants of *PWT3*, and Δ3Δ4 is a double disruptant of *PWT3* and *PWT4*.

involvement of a single gene was confirmed, *PWTX* was formally designated as *PWT7*.

For fine-mapping, we screened the whole BC_1F_1 population with the flanking markers MOAC3719 and MOAS347 and found a total of nine recombinants. Phenotyping of these recombinants revealed that *PWT7* was flanked by MOAC3719 and MOAC3166, with two recombinants each (Fig. 2B). We screened a bacterial artificial chromosome (BAC) library of Br58 genomic DNA with these flanking markers and found a BAC clone (ZA8-K1) containing both markers (Fig. 2C). ZA8-K1 was introduced into Br48, and the resulting seven transformants were subjected to infection assay with primary leaves. Of the seven, five transformants showed avirulence on Hope (Figs. 2C and 3A), indicating that this BAC clone harbors *PWT7*. These five transformants were also avirulent on CS and N4 (Fig. 3A), suggesting that *PWT7* is effective not only on Hope but also on CS and N4, as hypothesized in the infection assay with the *PWT3*- and *PWT4*-disruptants.

ZA8-K1 was sequenced with Illumina MiSeq, and the short reads obtained were assembled. The candidate region between MOAC3719 and MOAC3166 was covered by two contigs (contigs 2 and 3) with a small gap (Fig. 2C). On these contigs, we found eight putative genes encoding secreted proteins (F5, F39, F67, F57, F60, F64, F65, and F38) that were polymorphic between Br58 and Br48 and perfectly linked to *PWT7* (Fig. 2C). Fragments containing F5, F39+F67, F57, F60+F64+F65, and F38 were amplified with PCR, and the amplicons obtained (2,473, 4,967, 2,989, 4,131, and 2,664 bp, respectively) were cloned into pBluescript II SK(+). These clones were introduced into Br48, and the resulting transformants were sprayed onto primary leaves of test cultivars. Transformants carrying F38 (Supplementary Fig. S1) gained avirulence on Hope, CS, and N4 without losing virulence on Nigrate (Ngt) (a susceptible barley control) (Fig. 3A), while those carrying other candidate genes did not (Fig. 2C). From these results, we concluded that *PWT7* is F38, encoding a protein composed of 98 amino acids (Fig. 3B). As mentioned before, *PWT7* should be ineffective as an avirulence gene at the heading stage. To confirm this, one of the three transformants carrying F38 (Br48+PWT7) was sprayed onto spikes of Hope, CS, and N4. Br48+PWT7 was virulent on the spikes of these cultivars, as expected (Supplementary Fig. S2).

Distribution of *PWT7* in *Pyricularia* spp.

To survey the distribution of *PWT7* in *Pyricularia* spp., genomic DNA was extracted from 38 isolates of *P. oryzae* and its cryptic species, was digested with *Hin*dIII, and was hybridized with a plasmid clone containing a *PWT7*-ORF (open reading frame) fragment (384 bp) amplified from Br58. *PWT7* was ubiquitous in MoE (EC-II) and MoL, frequently detected in MoS, but completely absent in MoO, MoT, MoE (EC-I), and *Eragrostis* isolates (Supplementary Fig. S3; Supplementary Table S1). Most of the *PWT7* carriers had a single copy, but some MoL isolates had two copies (Supplementary Fig. S3). These homologs were amplified and directly sequenced. The MoS isolates with the positive signals shared a homolog with a 100% identical nucleotide sequence, which had four amino-acid substitutions compared with the authentic *PWT7* in Br58 (Fig. 3B). This homolog was designated as $PWT7^{Set}$. The MoE isolates with the positive signals shared another homolog with a 100% identical nucleotide sequence, which had one amino-acid substitution compared with the authentic *PWT7* (Fig. 3B). This homolog

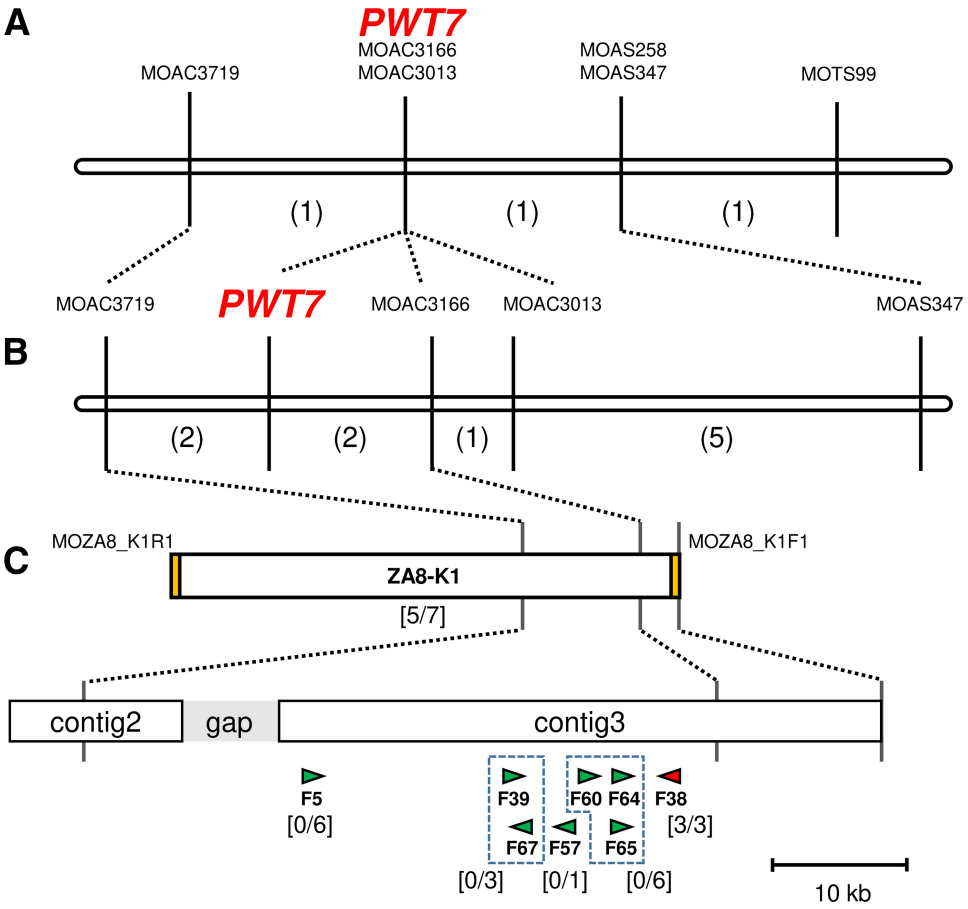

Fig. 2. Map-based cloning of *PWT7*. **A,** Genetic linkage map constructed using 79 BC_1F_1 cultures derived from 76Q1 × Br58. **B,** Fine map around *PWT7* constructed using a total of 167 BC_1F_1 cultures derived from 76Q1 × Br58. In A and B, numbers of recombinants are indicated in parentheses. **C,** A BAC clone spanning the candidate region and its nucleotide sequence contigs. Arrowheads indicate putative effector genes predicted with SignalP that were cloned into pBluescript II SK(+) and introduced into Br48. Genes enclosed in a dotted line were cloned together. Shown in square brackets are numbers of transformants avirulent on Hope and numbers of transformants tested.

was designated as *PWT7*^{Ele}. Most of the MoL isolates shared the third homolog with a 100% identical nucleotide sequence, which had four amino-acid substitutions compared with the authentic *PWT7* (Fig. 3B). This homolog corresponded to the 4.4-kb signal (Supplementary Fig. S3) and was designated as *PWT7*^{Lom}. The other copy (3.2 kb) in the MoL isolates carrying two copies was 100% identical in the nucleotide sequence and had one base substitution compared with *PWT7*^{Ele}. However, this homolog was identical to *PWT7*^{Ele} in the amino-acid sequence, since the base change was a synonymous substitution. Therefore, this homolog was designated as *PWT7*^{LomE}.

Functional analyses of *PWT7* homologs

To check the function of the homologs found in *P. oryzae*, *PWT7*^{Ele}, *PWT7*^{LomE}, *PWT7*^{Lom}, and *PWT7*^{Set} were amplified from MZ5-1-6 (MoE), TP1 (MoL), TP1, and GFSI1-7-2 (MoS), respectively, and amplicons (1,963, 773, 1,227, and 777 bp, respectively) were inserted into pBluescript II SK(+). These clones were introduced into Br48, and resulting transformants (Supplementary Fig. S1) were sprayed onto primary leaves of test cultivars. The transformants carrying *PWT7*^{Ele}, *PWT7*^{LomE}, and *PWT7*^{Lom} were avirulent on Hope, CS, and N4 (Fig. 3A), suggesting that they are functional. The transformant carrying *PWT7*^{Set} was avirulent on CS, moderately avirulent on Hope, but virulent on N4. This result suggests that *PWT7*^{Set} is basically functional but that its function is affected by alleles or genetic backgrounds of its corresponding resistance gene.

TP2 (MoL) is virulent on seedlings of Hope (Table 1) in spite of carrying a single copy of *PWT7*^{Lom}. Detailed analyses revealed that the expression of *PWT7*^{Lom} in TP2 was suppressed (Fig. 4B), probably due to an insertion of an LTR of transposable element Inago 1 (Sanchez et al. 2011) into its upstream region (Fig. 4A). This homolog in TP2 was designated as *PWT7*$^{Lom'}$.

Asuke et al. (2020b) suggested that the avirulence of MZ5-1-6 (MoE) on common wheat cultivars was controlled by at least five genes. Among the five, two (*eA1* and *eA2*) were effective on all three cultivars (CS, N4, and Hope), while the other three (*eA3*, *eA4*, and *eA5*) were effective on CS and N4 but not on Hope. The *eA3* gene was a *PWT3* homolog (Asuke et al. 2020b), while the *eA5* gene was designated as *PWT6* (Asuke et al. 2021). *PWT7* isolated in the present study is effective on all three cultivars, and therefore, should be *eA1* or *eA2*. To confirm it, a segregation analysis was performed using the F_1 cultures from MZ5-1-6 × Br48 reported by Asuke et al. (2020b). In this population, avirulent and virulent cultures segregated in a 3:1 ratio on Hope due to independent segregations of *eA1* and *eA2* (Asuke et al. 2020b). Genomic DNA was extracted from these F_1 cultures, and *PWT7*^{Ele} was amplified. Carriers and noncarriers segregated in a 1:1 ratio, and the carriers were all included in the cultures avirulent on Hope (Supplementary Fig. S4). Based on this result, we assigned *PWT7*^{Ele} to *eA1*.

Chromosomal locations of the *PWT7* homologs

As mentioned above, *PWT7*^{Ele} segregated in a 1:1 ratio in the F_1 population derived from MZ5-1-6 × Br48 (Table 2; Supplementary Fig. S4). This result suggests that *PWT7*^{Ele} is located on a core chromosome. An analysis of the whole-genome sequence of MZ5-1-6 (National Center for Biotechnology Information accession number GCA_004346975.1) revealed that *PWT7*^{Ele} is located on a subtelomeric region of chromosome 7 (Fig. 4A). Similarly, *PWT7*^{Set} segregated in a 1:1 ratio (Table 2) in the F_1 population from GFSI1-7-2 × Br48 produced by Chuma et al.

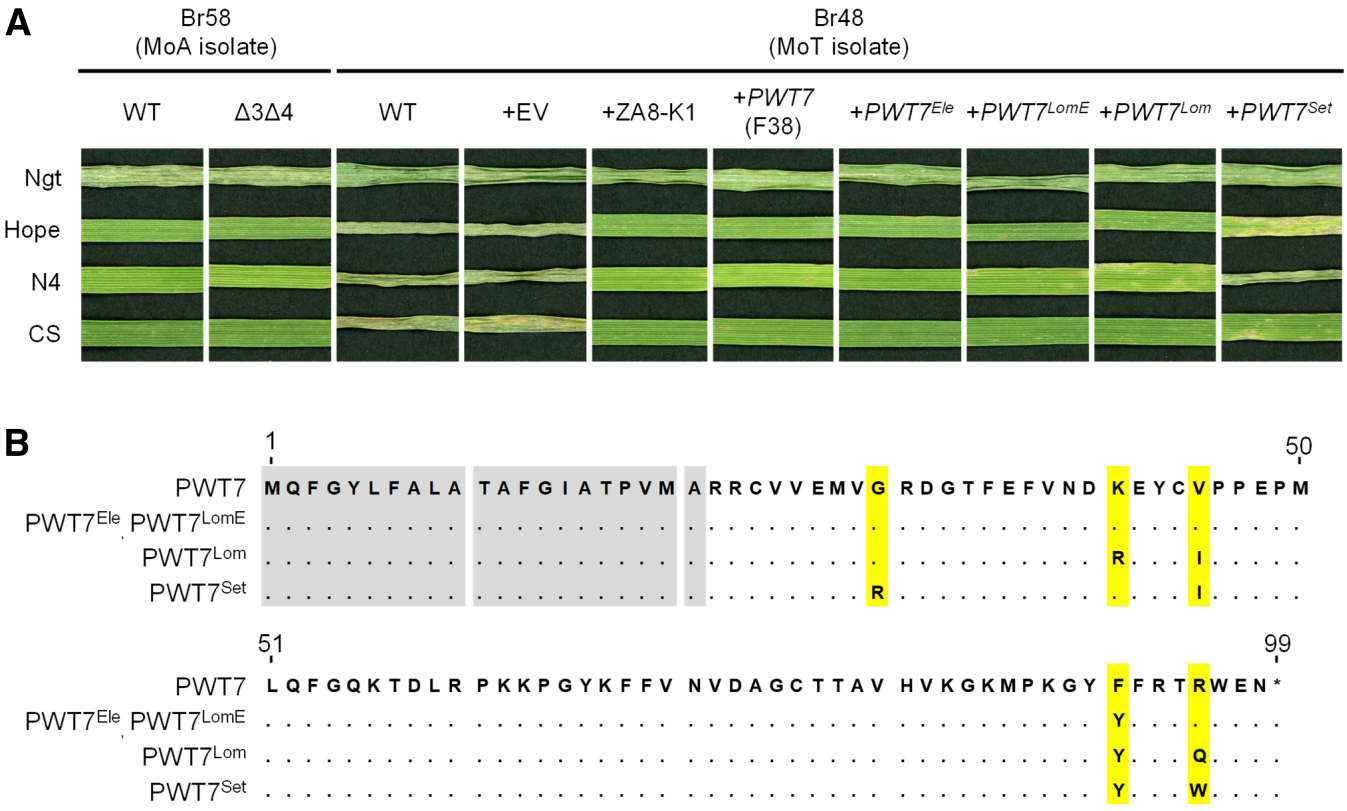

Fig. 3. Function and structures of *PWT7* and its homologs. **A,** Complementation tests with F38 (*PWT7*) and its homologs. Eight-day-old primary leaves of wheat cultivars Hope, N4, and CS were inoculated with MoA isolate Br58 (WT), its disruptant of *PWT3* and *PWT4* (Δ3Δ4), MoT isolate Br48 (WT), and its transformants carrying an empty vector (+EV), a BAC clone (+ZA8-K1), *PWT7* (+*PWT7*), *PWT7*^{Ele} (+*PWT7*^{Ele}), *PWT7*^{LomE} (+*PWT7*^{LomE}), *PWT7*^{Lom} (+*PWT7*^{Lom}), and *PWT7*^{Set} (+*PWT7*^{Set}). Barley cultivar Nigrate (Ngt) was used as a susceptible control. Phenotypes were evaluated 4 days after inoculation. **B,** Amino acid alignments of *PWT7* and its homologs. The predicted signal peptide and variable sites are indicated in gray and yellow, respectively.

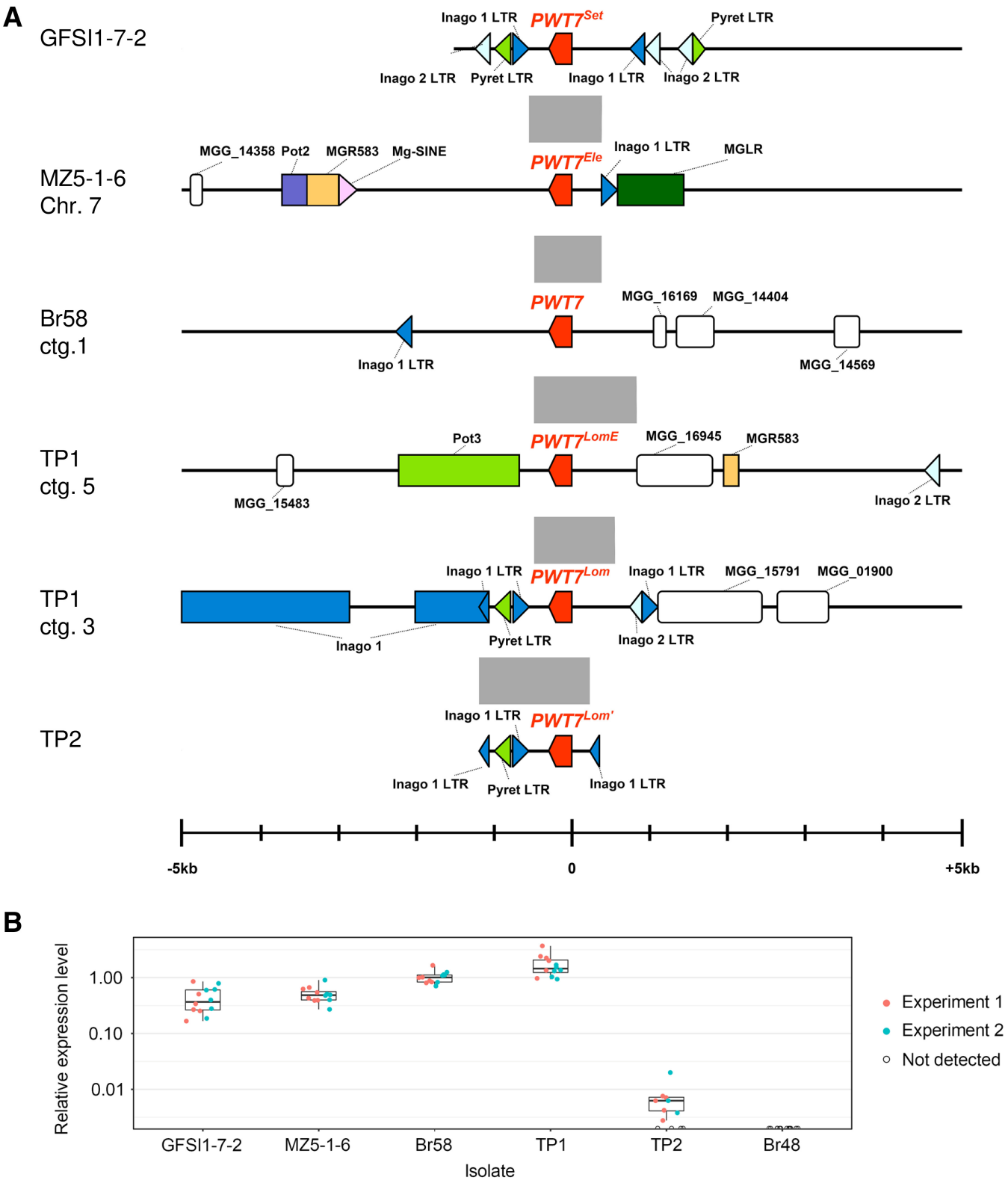

Fig. 4. Peripheral structures of *PWT7* homologs in various isolates and their expression. **A,** Structures around *PWT7* homologs in isolates from genera *Setaria* (GFSI1-7-2), *Eleusine* (MZ5-1-6), *Avena* (Br58), and *Lolium* (TP1, TP2). Shaded areas represent homologous regions. Red represents *PWT7* and its homologs, white represents single-copy genes, and the other colors represent repetitive elements. **B,** Expression levels of *PWT7* homologs of representative isolates in barley cultivar Nigrate, 24 h after inoculation. Relative gene expression levels were quantified using the comparative threshold ($2^{-\Delta\Delta Ct}$) method. β-Actin was used as internal control to normalize expression values, and the expression level of *PWT7* in Br58 was used as a calibrator. Data of 12 biological replicates from two independent experiments (six replicates per experiment) are shown as a boxplot with original data points. Center lines show the medians. Box limits indicate the 25th and 75th percentiles. Open circles indicate samples in which *PWT7* expression was not detected within 40 cycles in PCR.

(2010). This result suggests that *PWT7*^{Set} is also located on a core chromosome.

To examine the mode of inheritance of *PWT7* in Br58, a new F_1 population was produced by crossing Br58 with Br48. In this population the mating types segregated in a 1:1 ratio as expected (Table 2). However, the *PWT7* fragment was rarely amplified from genomic DNAs of the F_1 cultures (Table 2), indicating that *PWT7* is not inherited in a Mendelian manner. This result suggests that *PWT7* is located on a supernumerary chromosome.

Further, TP1Δ3 (Table 1), a carrier of *PWT7*^{Lom} and *PWT7*^{LomE}, was crossed with Br48. The resulting 90 F_1 cultures were subjected to Southern analysis so as to differentiate the two copies (*PWT7*^{Lom} and *PWT7*^{LomE}). Some examples are shown in Figure 5. In the F_1 population derived from TP1Δ3 × Br48, the two signals representing *PWT7*^{Lom} and *PWT7*^{LomE} were sporadically inherited, although the mating types were inherited in a Mendelian manner (Table 2). Furthermore, *PWT7*^{Lom} and *PWT7*^{LomE} were almost co-segregated; among the nine carriers (Table 2), seven cultures carried both homologs, although the other two carried *PWT7*^{Lom} alone (Fig. 5, #12) and *PWT7*^{LomE} alone (Fig. 5, #22). These results suggest that *PWT7*^{Lom} and *PWT7*^{LomE} are located on a supernumerary chromosome.

To confirm that *PWT7*, *PWT7*^{Lom}, and *PWT7*^{LomE} are located on supernumerary chromosomes, we sequenced genomic DNAs of Br58 and TP1 and generated near-complete genome assemblies. They were located on scaffolds that were not assembled to core chromosomes (Fig. 4A; Supplementary Fig. S5). Furthermore, *PWT7*^{Lom} and *PWT7*^{LomE} were located on the same scaffolds (chromosome Min1) of the LpKY97 genome (Rahnama et al. 2020) with a 465-kb interval, supporting the result from the segregation analysis, i.e., co-segregation of these two homologs. From these results, we conclude that *PWT7*, *PWT7*^{Lom}, and *PWT7*^{LomE} are located on supernumerary chromosomes. *PWT7*^{Set}, *PWT7*^{Ele}, *PWT7*^{LomE}, and *PWT7*^{Lom} were surrounded by transposable or repetitive elements (Fig. 4).

Discussion

Two avirulence genes, *PWT3* and *PWT4*, were found in *Avena* isolate Br58, based on segregation analyses of an F_1 population derived from Br58 × Br48 (Takabayashi et al. 2002). In the present study, we found an additional avirulence gene, *PWT7*, in Br58. A question is why Takabayashi et al. (2002) could not find *PWT7* in their segregation analyses. The present study suggests that this is because *PWT7* is located on a supernumerary chromosome. Actually, in the 77 F_1 cultures they produced, *PWT7* carriers were only four and were included in *PWT3* carriers. Therefore, the avirulence conferred by *PWT7* was masked by the avirulence conferred by *PWT3*. The second question is why the linkage analysis was possible in the next (BC_1F_1) generation. Luo et al. (2007) reported that a supernumerary chromosome carrying a portion of a core chromosome was inherited in a Mendelian fashion. Kusaba et al. (2014) reported that an avirulence gene was translocated from a supernumerary chromosome to a core chromosome in a genetic cross. We suggest that 76Q1, an F_1 culture derived from Br58 × Br48, has a chimeric chromosome resulting from a translocation of a chromosomal segment between the supernumerary chromosome and a core chromosome, which made it possible to perform a linkage analysis in the BC_1F_1 generation.

PWT7^{Ele} was one (*eA1*) of the five genes (Asuke et al. 2020b) controlling the avirulence of MZ5-1-6 (MoE) on wheat. We have already identified or characterized two other avirulence genes of the five, i.e., *PWT3* (*eA3*) and *PWT6* (*eA5*) (Asuke et al. 2020b, 2021). These three genes were plotted on phylogenetic networks of 80 representative isolates constructed using SNPs in their whole-genome sequences (Fig. 6). *PWT6* homologs were present in MoE isolates but completely absent in the clade

Table 2. Segregation of mating types and *PWT7* homologs in random F_1 populations derived from crosses among pathotypes

	Mating type				*PWT7* homologs			
	No. of F_1 cultures				No. of F_1 cultures			
Cross	*MAT1-2*	*MAT1-1*	Total	x^2 (1:1)[b]	Carrier[a]	Noncarrier	Total	x^2 (1:1)[b]
GFSI1-7-2 (*MAT1-2*; *PWT7*^{Set}) × Br48 (*MAT1-1*)	38	32	70	0.51	39	31	70	0.91
MZ5-1-6 (*MAT1-2*; *PWT7*^{Ele}) × Br48 (*MAT1-1*)	36	44	80	0.80	40	40	80	0.00
Br58 (*MAT1-2*; *PWT7*) × Br48 (*MAT1-1*)	16	17	33	0.03	1	32	33	29.12**
TP1Δ3 (*MAT1-2*; *PWT7*^{Lom}; *PWT7*^{LomE}) × Br48 (*MAT1-1*)	48	42	90	0.40	9	81	90	57.60**

[a] In the F_1 population derived from TP1Δ3 × Br48, cultures carrying at least one homolog are counted.
[b] Significant at the 5% (*) and 1% (**) levels.

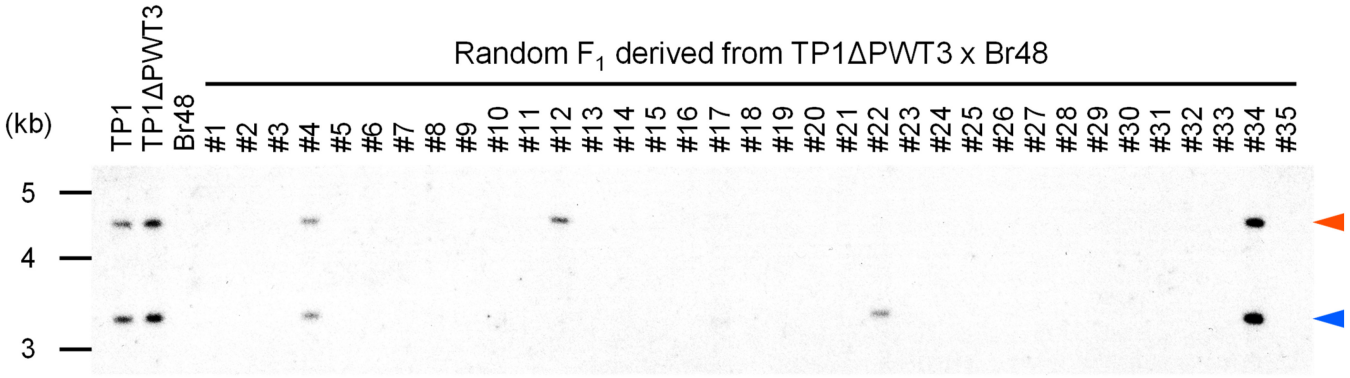

Fig. 5. Inheritance of *PWT7* homologs in F_1 cultures derived from a cross between TP1ΔPWT3 and Br48. Genomic DNA was digested with *Hin*dIII and was electrophoresed, blotted, and hybridized with pBluescript II SK(+) containing the *PWT7* open reading fragment. Red and blue arrowheads indicate signals of *PWT7*^{Lom} (4.4 kb) and *PWT7*^{LomE} (3.2 kb), respectively.

consisting of MoL, MoA, and MoT isolates (tentatively designated as the 'LAT clade'). In the LAT clade, *PWT7* homologs were present in most of MoL and MoA isolates but completely absent in MoT isolates. Functional *PWT3* homologs were present in MoL, MoA, and a small portion of MoT isolates but absent in most MoT isolates. The MoT isolates carrying the functional *PWT3* were those collected within seven years after the first wheat blast outbreak in Brazil in 1985 and are considered to be colonizing wheat cultivars lacking *Rwt3* (Inoue et al. 2017). These results suggest that, in the course of parasitic specialization toward MoT, a common ancestor of MoE, MoL, MoA, and MoT first lost *PWT6*, secondly *PWT7*, and finally, the function of *PWT3*. Tosa (1992) proposed a model illustrating the evolution of formae speciales of *Blumeria graminis* as a process of functional losses of avirulence genes. In the present study, we could illustrate the loss process of *PWT7,* the third *P. oryzae* avirulence gene involved in the evolution toward MoT. Cloning of the remaining two avirulence genes (*eA2* and *eA4*) will make it possible to elucidate the whole process of evolution from the common ancestor of MoE, MoL, and MoA to MoT.

Wheat blast is known as a spike disease because its initial identifiable or most distinguishable symptoms are observed on spikes (Singh et al. 2021). Therefore, the gain of pathogenicity on wheat spikes may be enough for the blast fungus to survive on wheat. However, all MoT isolates tested were noncarriers of *PWT7*, an avirulence gene effective only on seedlings or leaves. Considering that most of MoL and MoA isolates, close relatives of MoT, are *PWT7* carriers, an ancestor of MoT is assumed to have lost *PWT7* in the process of evolution toward MoT. We suggest that overcoming the seedling resistance through the loss of *PWT7* was a prerequisite for the establishment of MoT. The loss of *PWT7* may have contributed to an enhancement of infectivity through increase of inocula (conidia) produced on seedlings and leaves or may have made it possible for mycelia to grow internally from infected seeds to spikes through seedlings and culms.

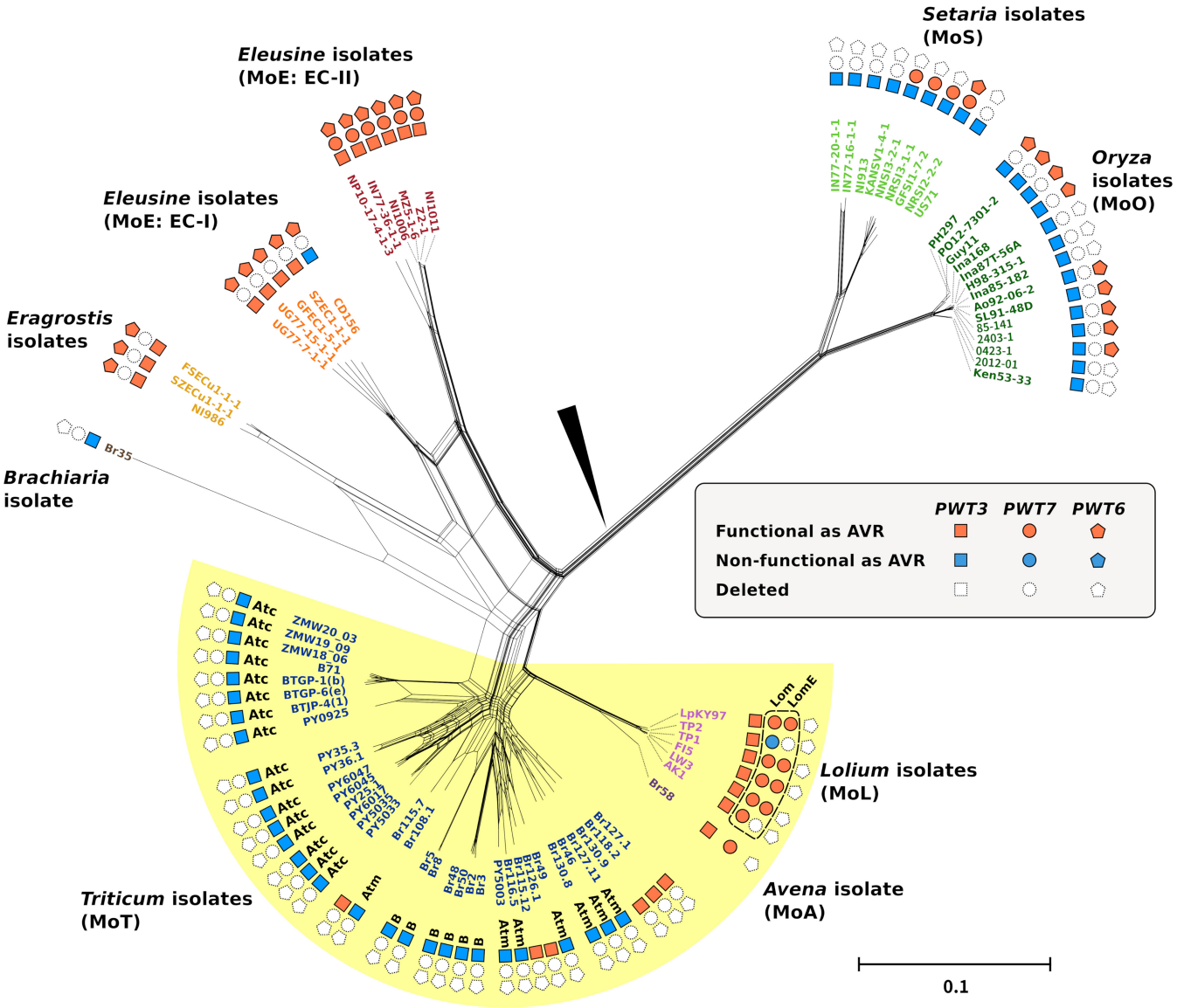

Fig. 6. Distribution of *PWT3*, *PWT6*, and *PWT7* in *Pyricularia oryzae*. The presence or absence of functional or nonfunctional homologs of these avirulence genes was plotted on a Neighbor-Net network constructed with SplitsTree software, using the whole-genome 643,804 biallelic single nucleotide polymorphism sites. The arrowhead indicates the node to the outgroup taxon (*Pyricularia grisea* Dig41) inferred by Asuke et al. (2020a). Atm, B, and Atc are nonfunctional *PWT3* alleles reported by Inoue et al. (2017). The LAT clade is shaded in yellow.

PWT7 is located on core chromosomes in MZ5-1-6 (MoE) and GFSI1-7-2 (MoS) but on supernumerary chromosomes in TP1 (MoL) and Br58 (MoA). This is an example of interchromosomal translocations of effector genes between core and supernumerary chromosomes (Langner et al. 2021; Peng et al. 2019). It should be noted that supernumerary chromosomes are ubiquitous in MoL isolates but absent in MoT isolates collected soon after the emergence of wheat blast (Langner et al. 2021; Peng et al. 2019). This fact may offer a clue to how the direct ancestor of MoT lost *PWT7*. Supernumerary chromosomes are frequently lost during meiosis and mitosis (Peng et al. 2019). The MoL population already contains some isolates that lost *PWT7* (Fig. 6; Supplementary Fig. S3). Such noncarriers may have become an ancestor of MoT. Alternatively, the common ancestor or ancestors may have lost their supernumerary chromosomes as a result of sexual reproduction, which was suggested to have been common in the early days of the wheat blast epidemic (Cruz and Valent 2017; Langner et al. 2021). Further studies are needed to elucidate mechanisms of the loss of *PWT7*.

Materials and Methods

Fungal materials

Pyricularia oryzae isolates analyzed in the present study are listed in Supplementary Table S1. To produce the 167 random BC_1F_1 cultures for mapping of *PWTX* (*PWT7*), 76Q1, one of the random F_1 cultures derived from Br58 (MoA isolate) × Br48 (MoT isolate) (Takabayashi et al. 2002), was backcrossed with Br58 on oatmeal agar media, as described previously (Murakami et al. 2000). To examine modes of inheritance of *PWT7*, Br58 and TP1ΔPWT3 (*PWT7* carriers) were crossed with Br48 (lacking *PWT7*). TP1ΔPWT3 is a *PWT3* disruptant of TP1 (MoL isolate) described below. The resulting two F_1 populations (composed of 33 and 90 random cultures, respectively) were subjected to segregation analyses of *PWT7*. The mode of inheritance of *PWT7* was also examined by using the 80 random F_1 cultures derived from MZ5-1-6 (MoE isolate) × Br48 produced by Asuke et al. (2020b) and the 70 random F_1 cultures derived from GFSI1-7-2 (MoS isolate) × Br48 produced by Chuma et al. (2010). Mating types and *PWT7* genotypes of these F_1 cultures were determined by PCR, using QuickTaq (Toyobo) with primer pairs A1/A5 and PWT7-ORF-F/PWT7-ORF-R, respectively (Supplementary Table S2).

Plant materials

Hope, N4, and CS, three common wheat (*Triticum aestivum*) cultivars, were used for infection assay at the seedling and heading stages. A barley cultivar (*Hordeum vulgare*), Ngt, was used as a susceptible control.

Transformation of *P. oryzae*

A BAC library of Br58 genomic DNA was constructed using the pcc1BAC/*Bam*HI vector (Epicentre) and was screened with linked markers. A large plasmid DNA of ZA8-K1, a clone containing the candidate region of *PWTX* (*PWT7*), was extracted using NucleoBond Xtra BAC (Macherey-Nagel). Fragments containing *PWT7*, $PWT7^{Ele}$, $PWT7^{LomE}$, $PWT7^{Lom}$, and $PWT7^{Set}$ (2,664, 1,963, 773, 1,227, and 777 bp in size, respectively) were amplified from genomic DNA of Br58, MZ5-1-6, TP1, TP1, and GFSI1-7-2, with KOD One PCR master mix (Toyobo) and primers shown in Supplementary Table S2. Each fragment was cloned into pBluescript II SK(+). The BAC clone and these recombinant plasmids were introduced into Br48 by the polyethylene glycol–mediated co-transformation with pSH75 carrying a hygromycin B phosphotransferase gene, as described by Tosa et al. (2005). Introduced *PWT7* was confirmed by PCR, using the PWT7-ORF primers (Supplementary Table S2). *PWT3* disruptants (Table 1) of four MoL isolates (TP1, AK1, LW3, FI5) were produced with a split marker method, as described by Inoue et al. (2017).

Pathogenicity assay at the seedling stage

Wheat and barley seeds were sown in vermiculite supplied with the liquid fertilizer Hyponex (diluted 1,500 times with water) (Hyponex) in a seeding case (5.5 × 15 × 10 cm) and were grown at 22°C with a 12-h photoperiod of fluorescent lighting for 8 days. Primary leaves of the seedlings were fixed onto a plastic board with rubber bands just before inoculation. Conidial suspensions (1×10^5 conidia per milliliter) containing 0.01% Tween20, prepared as described by Tagle et al. (2015), were sprayed on primary leaves, using an air compressor. The inoculated seedlings were incubated in the darkness in high-humidity trays for 24 h at 22°C, then, were transferred to a dry condition with a 12-h photoperiod of fluorescent lighting at 22°C. Four to 6 days after inoculation, symptoms were evaluated on the basis of the size and color of lesions. The size was rated on six grades from 0 to 5: 0 = no visible lesions, 1 = pinhead spots, 2 = small lesions (<1.5 mm), 3 = scattered lesions of intermediate size (<3 mm), 4 = large typical lesion, and 5 = complete shriveling of leaf blades. Infection types comprised a number indicating the lesion size and a letter denoting the lesion color, 'B' for brown and 'G' for green. Infection types 0 to 5 with B were considered resistant, whereas infection types 3 to 5 with G were considered susceptible. Assays at the seedling stage were conducted three times.

Pathogenicity assay at the heading stage

Wheat cultivars Hope, N4, and CS were grown for approximately five months in a field at Kobe University. At the heading stage, culms bearing spikes at full emergence (but before anthesis) were cut and trimmed to approximately 40 cm and were put into a test tube with water containing antibiotics (Misaki solution for cut flowers; OAT Agrio). The spikes were inoculated with conidial suspension (1.0×10^5 conidia per milliliter) containing 0.01% Tween20, were covered with plastic bags, and were incubated in darkness, at 25°C, in the growth chamber. The plastic bags were removed 24 h after inoculation, and the spikes were further incubated for 7 to 10 days, under a 12-h photoperiod, at 25°C. Blast reactions were scored with six progressive grades: 0 = no visible infection, 1 = pinhead spots, 2 = small lesions (<1.5 mm), 3 = scattered lesions of intermediate size (<3 mm), 4 = mixture of green and white tissues with no apparent browning caused by hypersensitivity, and 5 = complete blighting of the spike. Infection types 0 to 3 were considered resistant and 4 to 5 were considered susceptible (Tagle et al. 2015). Assays at the heading stage were conducted three times.

Distribution analysis of *PWT7* by Southern hybridization

Genomic DNAs of representative isolates and strains of *P. oryzae* were extracted from mycelia grown in complete liquid media, as described by Nakayashiki et al. (1999). Extracted DNAs were digested with *Hin*dIII (New England Biolabs) at 37°C overnight, were electrophoresed on 0.7% agarose gels in Tris-borate-EDTA buffer for 15 h at 30 V, and were blotted to Hybond N^+ membranes (GE Healthcare). A 384-bp fragment containing an ORF of *PWT7* was amplified from the genomic DNA of Br58 with PWT7-ORF forward and reverse primers (Supplementary Table S2) and KOD One (Toyobo), using Mastercycler (Eppendolf). The amplicon was cloned into the *Eco*RV site of pBluescript II SK(+) using the DNA ligation kit, ver.2.1 (Takara). The membrane was hybridized with the labeled recombinant plasmid using the ECL direct nucleic acid labeling and detection system (GE Healthcare), according to manufacturer instructions.

Expression analysis of *PWT7*

To verify expression levels of *PWT7* homologs, comparative expression analysis was performed using real-time quantitative PCR (qPCR). Nine-day-old primary leaves of Ngt were inoculated with Br58 (*PWT7*), MZ5-1-6 ($PWT7^{Ele}$), TP1 ($PWT7^{LomE}$ and $PWT7^{Lom}$), TP2 ($PWT7^{Lom'}$), GFSI1-7-2 ($PWT7^{Set}$), and Br48 (−) and were incubated for 24 h. Total RNA was extracted from the inoculated leaves with Sepasol-RNA I Super G (Nacalai Tesque) and were treated with DNase I at 37°C for 20 min. Complementary DNA was synthesized using PrimeScript RT master mix (Perfect Real Time) (Takara), according to manufacturer instructions. qPCR was performed using Applied Biosystems QuantStudio 1 with FastStart Universal SYBR Green Master (Rox) (Roche Diagnostics). Forward and reverse primers for *PWT7* (target gene) and the actin gene (internal control) were Exp-PWT7 and Exp-Actin, respectively (Supplementary Table S2). Relative changes in *PWT7* expression values were calculated using the $2^{-\Delta\Delta Ct}$ (ΔCt) method (Livak and Schmittgen 2001). The average ΔCt value of Br58 was chosen as the calibrator.

De novo assembly of Nanopore long reads of Br58 and TP1 genomes

High–molecular weight genomic DNAs of Br58 and TP1 were extracted from mycelia using NucleoBond HMW DNA (Macherey-Nagel). Sequencing adapters were ligated using a Ligation Sequencing kit LSK110 according to the 1D protocol from Oxford Nanopore. Resulting libraries were then sequenced on MinION R9.4 flow cells (Oxford Nanopore Technologies). Generated Nanopore long reads were assembled into contigs using NECAT (Chen et al. 2021) and, then, were polished using Nextpolish with their Illumina short reads.

Comparison of genomic regions harboring *PWT7* and its homologs

Genomic sequences around *PWT7*, $PWT7^{LomE}$, $PWT7^{Lom}$, and $PWT7^{Ele}$ (5 kb up- and downstream from their start codons) were extracted from the long read assembly of Br58, TP1, TP1, and MZ5-1-6 (Gómez Luciano et al. 2019), respectively. Those around $PWT7^{Set}$ and $PWT7^{Lom'}$ were extracted from assemblies of Illumina short reads of GFSI1-7-2 and TP2, respectively, and were constructed using SPAdes (Bankevich et al. 2012). Sequence similarities were calculated using the BLASTN program, implemented in Easyfig version 2.1 (Sullivan et al. 2011). Genes and transposons in each genomic sequence were identified by BLASTN (BLAST+2.6.0 https://www.ncbi.nlm.nih.gov/blast), using known transposable elements and a gene set of 70-15 (Dean et al. 2005) as a query sequence.

Phylogenetic analysis

Whole genome sequence reads of the 80 isolates listed in Supplementary Table S1, with accession numbers, were used for phylogenetic analysis. A total of 41 isolates were sequenced in the present study, including three *Oryza* isolates, eight *Setaria* isolates, three *Eragrostis* isolates, eight *Eleusine* isolates, four *Lolium* isolates, and 15 *Triticum* isolates. Genomic DNA was extracted with the NucleoSpin Plant II (Macherey-Nagel), according to manufacturer instructions. Sequencing libraries were generated using a NEBNext Ultra II DNA library prep kit for Illumina (New England Biolabs). The library of TP1 was sequenced using Illumina Miseq, while the other libraries were sequenced using Illumina NovaSeq 6000. Sequenced short reads were mapped to the genome assembly of MZ5-1-6 (Gómez Luciano et al. 2019), using BWA version 0.7.17 (Li and Durbin 2010). Alignments were sorted with samtools version 1.9 (Li et al. 2009). The Genome Analysis Toolkit, version 4.1.4.1 (McKenna et al. 2010), was used for calling SNPs and indels as described by Asuke et al. (2021). A phylogenetic network was constructed using SplitsTree 4.18.1 (Huson and Bryant 2006), based on biallelic SNPs. Alleles of *PWT7*, *PWT3*, and *PWT6* in each genome was confirmed by BLAST+2.6.0.

Acknowledgments

We thank K. Sato and H. Hisano, Okayama University, for valuable discussions in a project including the present study. Computations were partially performed on the National Institute of Genetics supercomputer at the Research Organization of Information and Systems.

Literature Cited

Abe, A., Kosugi, S., Yoshida, K., Natsume, S., Takagi, H., Kanzaki, H., Matsumura, H., Yoshida, K., Mitsuoka, C., Tamiru, M., Innan, H., Cano, L., Kamoun, S., and Terauchi, R. 2012. Genome sequencing reveals agronomically important loci in rice using MutMap. Nat. Biotechnol. 30:174-178.

Asuke, S., Magculia, N. J., Inoue, Y., Vy, T. T. P., and Tosa, Y. 2021. Correlation of genomic compartments with contrastive modes of functional losses of host specificity determinants during pathotype differentiation in *Pyricularia oryzae*. Mol. Plant-Microbe Interact. 34:680-690.

Asuke, S., Nishimi, S., and Tosa, Y. 2020b. At least five major genes are involved in the avirulence of an *Eleusine* isolate of *Pyricularia oryzae* on common wheat. Phytopathology 110:465-471.

Asuke, S., Tanaka, M., Hyon, G. S., Inoue, Y., Vy, T. T. P., Niwamoto, D., Nakayashiki, H., and Tosa, Y. 2020a. Evolution of an *Eleusine*-specific subgroup of *Pyricularia oryzae* through a gain of an avirulence gene. Mol. Plant-Microbe Interact. 33:153-165.

Bankevich, A., Nurk, S., Antipov, D., Gurevich, A. A., Dvorkin, M., Kulikov, A. S. Lesin, V. M., Nikolenko, S. I., Pham, S., Prjibelski, A. D., Pyshkin, A. V., Sirotkin, A. V., Vyahhi, N., Tesler, G., Alekseyev, M. A., and Pevzner, P. A. 2012. SPAdes: A new genome assembly algorithm and its applications to single-cell sequencing. J. Comput. Biol. 19: 455-477.

Chen, Y., Nie, F., Xie, S. Q., Zheng, Y. F., Dai, Q., Bray, T. W., Y., X., Xing, J. F., Huang, Z. J., Wang, D. P., He, L. J., Luo, F., Wang, J. X., Liu, Y. Z., and Xiao, C. L. 2021. Efficient assembly of nanopore reads via highly accurate and intact error correction. Nat. Commun. 12:60.

Chuma, I., Zhan, S., Asano, S., Nga, N. T. T., Vy, T. T. P., Shirai, M., Ibaragi, K., and Tosa, Y. 2010. *PWT1*, an avirulence gene of *Magnaporthe oryzae* tightly linked to the rDNA locus, is recognized by two staple crops, common wheat and barley. Phytopathology 100:436-443.

Cruz, C. D., and Valent, B. 2017. Wheat blast disease: Danger on the move. Trop. Plant Pathol. 42:210-222.

Dean, R. A., Talbot, N. J., Ebbole, D. J., Farman, M. L., Mitchell, T. K., Orbach, M. J., Thon, M., Kulkarni, R., Xu, J. R., Pan, H., Read, N. D., Lee, Y. H., Carbone, I., Brown, D., Oh, Y. Y., Donofrio, N., Jeong, J. S., Soanes, D. M., Djonovic, S., Kolomiets, E., Rehmeyer, C., Li, W., Harding, M., Kim, S., Lebrun, M. H., Bohnert, H., Coughlan, S., Butler, J., Calvo, S., Ma, L. J., Nicol, R., Purcell, S., Nusbaum, C., Galagan, J. E., and Birren, B. W. 2005. The genome sequence of the rice blast fungus *Magnaporthe grisea*. Nature 434:980-986.

Gladieux, P., Condon, B., Ravel, S., Soanes, D., Maciel, J. L. N., Nhani, A., Chen, L., Terauchi, R., Lebrun, M. H., Tharreau, D., Mitchell, T., Pedley, K. F., Valent, B., Talbot, N. J., Farman, M., and Fournier, E. 2018. Gene flow between divergent cereal- and grass-specific lineages of the rice blast fungus *Magnaporthe oryzae*. mBio 9:e01219-17.

Gómez Luciano, L. B., Tsai, I. J., Chuma, I., Tosa, Y., Chen, Y.-H., Li, J.-Y., Li, M.-Y., Lu, M.-Y. J., Nakayashiki, H., and Li, W.-H. 2019. Blast fungal genomes show frequent chromosomal changes, gene gains and losses, and effector gene turnover. Mol. Biol. Evol. 36:1148-1161.

Huson, D. H., and Bryant, D. 2006. Application of phylogenetic networks in evolutionary studies. Mol. Biol. Evol. 23:254-267.

Inoue, Y., Vy, T. T. P., Yoshida, K., Asano, H., Mitsuoka, C., Asuke, S., Anh, V. L., Cumagun, C. J. R., Chuma, I., Terauchi, R., Kato, K., Mitchell, T., Valent, B., Farman, M., and Tosa, Y. 2017. Evolution of the wheat blast fungus through functional losses in a host specificity determinant. Science 357:80-83.

Islam, M. T., Croll, D., Gladieux, P., Soanes, D. M., Persoons, A., Bhattacharjee, P., Hossain, M. S., Gupta, D. R., Rahman, M. M., Mahboob, M. G., Cook, N., Salam, M. U., Surovy, M. Z., Sancho, V. B., Maciel, J. L., NhaniJúnior, A., Castroagudín, V. L., Reges, J. T., Ceresini, P. C., Ravel, S., Kellner, R., Fournier, E., Tharreau, D., Lebrun, M. H., McDonald, B. A., Stitt, T., Swan, D., Talbot, N. J., Saunders, D. G., Win, J., and Kamoun, S. 2016. Emergence of wheat blast in Bangladesh was

caused by a South American lineage of *Magnaporthe oryzae*. BMC Biol. 14:84.

Kato, H., Yamamoto, M., Yamaguchi-Ozaki, T., Kadouchi, H., Iwamoto, Y., Nakayashiki, H., Tosa, Y., Mayama, S., and Mori, N. 2000. Pathogenicity, mating ability and DNA restriction fragment length polymorphisms of *Pyricularia* populations isolated from Gramineae, Bambusideae and Zingiberaceae plants. J. Gen. Plant Pathol. 66:30-47.

Kusaba, M., Mochida, T., Naridomi, T., Fujita, Y., Chuma, I., and Tosa, Y. 2014. Loss of a 1.6 Mb chromosome in *Pyricularia oryzae* harboring two alleles of *AvrPik* leads to acquisition of virulence to rice cultivars containing resistance alleles at the *Pik* locus. Curr. Genet. 60:315-325.

Langner, T., Harant, A., Gomez-Luciano, L. B., Shrestha, R. K., Malmgren, A., Latorre, S. M., Burbano, H. A., Win, J., and Kamoun, S. 2021. Genomic rearrangements generate hypervariable mini-chromosomes in host-specific isolates of the blast fungus. PLoS Genet. 17:e1009386.

Latorre, S. M., Were, V. M., Foster, A. J., Langner, T., Malmgren, A., Harant, A., Asuke, S., Reyes-Avila, S., Gupta, D. R., Jensen, C., Ma, W., Mahmud, N. U., Mehebub, M. S., Mulenga, R. M., Muzahid, A. N. M., Paul, S. K., Rabby, S. M. F., Rahat, A. A. M., Ryder, L., Shrestha, R.-K., Sichilima, S., Soanes, D. M., Singh, P. K., Bentley, A. R., Saunders, D. G. O., Tosa, Y., Croll, D., Lamour, K. H., Islam, T., Tembo, B., Win, J., Talbot, N. J., Burbano, H. A., and Kamoun, S. 2023. Genomic surveillance uncovers a pandemic clonal lineage of the wheat blast fungus. PLoS Biol. 21:e3002052.

Li, H., and Durbin, R. 2010. Fast and accurate long-read alignment with Burrows-Wheeler transform. Bioinformatics 26:589-595.

Li, H., Handsaker, B., Wysoker, A., Fennell, T., Ruan, J., Homer, N., Marth, G., Abecasis, G., and Durbin, R. 2009. The sequence alignment/map format and SAMtools. Bioinformatics 25:2078-2079.

Livak, K. J., and Schmittgen, T. D. 2001. Analysis of relative gene expression data using real-time quantitative PCR and the $2^{-\Delta\Delta C(T)}$ method. Methods 25:402-408.

Luo, C.-X., Yin, L.-F., Ohtaka, K., and Kusaba, M. 2007. The 1.6 Mb chromosome carrying the avirulence gene *AvrPik* in *Magnaporthe oryzae* isolate 84R-62B is a chimera containing chromosome 1 sequences. Mycol. Res. 111:232-239.

McKenna, A., Hanna, M., Banks, E., Sivachenko, A., Cibulskis, K., Kernytsky, A., Garimella, K., Altshuler, D., Gabriel, S., Daly, M., and DePristo, M. A. 2010. The genome analysis toolkit: A MapReduce framework for analyzing next-generation DNA sequencing data. Genome Res. 20:1297-1303.

Murakami, J., Tosa, Y., Kataoka, T., Tomita, R., Kawasaki, J., Chuma, I., Sesumi, Y., Kusaba, M., Nakayashiki, H., and Mayama, S. 2000. Analysis of host species specificity of *Magnaporthe grisea* toward wheat using a genetic cross between isolates from wheat and foxtail millet. Phytopathology 90:1060-1067.

Nakayashiki, H., Kiyotomi, K., Tosa, Y., and Mayama, S. 1999. Transposition of the retrotransposon MAGGY in heterologous species of filamentous fungi. Genetics 153:693-703.

Oh, H. S., Tosa, Y., Takabayashi, N., Nakagawa, S., Tomita, R., Don, L. D., Kusaba, M., Nakayashiki, H., and Mayama, S. 2002. Characterization of an *Avena* isolate of *Magnaporthe grisea* and identification of a locus conditioning its specificity on oat. Can. J. Bot. 80:1088-1095.

Peng, Z., Oliveira-Garcia, E., Lin, G., Hu, Y., Dalby, M., Migeon, P., Tang, H., Farman, M., Cook, D., White, F. F., Valent, B., and Liu, S. 2019. Effector gene reshuffling involves dispensable mini-chromosomes in the wheat blast fungus. PLoS Genet. 15:e1008272.

Rahnama, M., Novikova, O., Starnes, J. H., Zhang, S., Chen, L., and Farman, M. L. 2020. Transposon-mediated telomere destabilization: A driver of genome evolution in the blast fungus. Nucleic Acids Res. 48: 7197-7217.

Sanchez Jr., E., Asano, K., and Sone, T. 2011. Characterization of *Inago1* and *Inago2* retrotransposons in *Magnaporthe oryzae*. J. Gen. Plant Pathol. 77:239-242.

Singh, P. K., Gahtyari, N. C., Roy, C., Roy, K. K., He, X., Tembo, B., Xu, K., Juliana, P., Sonder, K., Kabir, M. R., and Chawade, A. 2021. Wheat blast: A disease spreading by intercontinental jumps and its management strategies. Front. Plant Sci. 12:710707.

Sullivan, M. J., Petty, N. K., and Beatson, S. A. 2011. Easyfig: A genome comparison visualizer. Bioinformatics 27:1009-1010.

Tagle, A. G., Chuma, I., and Tosa, Y. 2015. *Rmg7*, a new gene for resistance to *Triticum* isolates of *Pyricularia oryzae* identified in tetraploid wheat. Phytopathology 105:495-499.

Takabayashi, N., Tosa, Y., Oh, H. S., and Mayama, S. 2002. A gene-for-gene relationship underlying the species-specific parasitism of *Avena/Triticum* isolates of *Magnaporthe grisea* on wheat cultivars. Phytopathology 92:1182-1188.

Tembo, B., Mulenga, R. M., Sichilima, S., M'siska, K. K., Mwale, M., Chikoti, P. C., Singh, P. K., He, X., Pedley, K. F., Peterson, G. L., Singh, R. P., and Braun, H. J. 2020. Detection and characterization of fungus (*Magnaporthe oryzae* pathotype *Triticum*) causing wheat blast disease on rain-fed grown wheat (*Triticum aestivum* L.) in Zambia. PLoS One 15:e0238724.

Tosa, Y. 1992. A model for the evolution of formae speciales and races. Phytopathology 82:728-730.

Tosa, Y., Hirata, K., Tamba, H., Nakagawa, S., Chuma, I., Isobe, C., Osue, J., Urashima, A. S., Don, L. D., Kusaba, M., Nakayashiki, H., Tanaka, A., Tani, T., Mori, N., and Mayama, S. 2004. Genetic constitution and pathogenicity of *Lolium* isolates of *Magnaporthe oryzae* in comparison with host species-specific pathotypes of the blast fungus. Phytopathology 94:454-462.

Tosa, Y., Osue, J., Eto, Y., Oh, H. S., Nakayashiki, H., Mayama, S., and Leong, S. A. 2005. Evolution of an avirulence gene *AVR1-CO39* concomitant with the evolution and differentiation of *Magnaporthe oryzae*. Mol. Plant-Microbe Interact. 18:1148-1160.

Urashima, A. S., Igarashi, S., and Kato, H. 1993. Host range, mating type, and fertility of *Pyricularia grisea* from wheat in Brazil. Plant Dis. 77:1211-1216.

Vy, T. T. P., Hyon, G.-S., Nga, N. T. T., Inoue, Y., Chuma, I., and Tosa, Y. 2014. Genetic analysis of host-pathogen incompatibility between *Lolium* isolates of *Pyricularia oryzae* and wheat. J. Gen. Plant Pathol. 80: 59-65.